



University of Warwick institutional repository: <http://go.warwick.ac.uk/wrap>

This paper is made available online in accordance with publisher policies. Please scroll down to view the document itself. Please refer to the repository record for this item and our policy information available from the repository home page for further information.

To see the final version of this paper please visit the publisher's website. Access to the published version may require a subscription.

Author(s): N. R. Deacon, P. J. Groot, J. E. Drew, R. Greimel, N. C. Hambly, M. J. Irwin, A. Aungwerojwit, J. Drake, D. Steeghs
Article Title: The IPHAS-POSS-I proper motion survey of the Galactic plane
Year of publication: 2009

Link to published article:

<http://link.aps.org/doi/10.1111/j.1365-2966.2009.15077.x>

Publisher statement: The definitive version is available at www.blackwellsynergy.com

The IPHAS-POSS-I proper motion survey of the Galactic Plane

N.R. Deacon^{*1}, P.J. Groot¹, J.E. Drew², R. Greimel^{3,4}, N.C. Hambly⁵, M.J. Irwin⁶,
A. Aungwerojwit^{7,8}, J. Drake⁹, D. Steeghs^{8,9},

¹*Department of Astrophysics, IMAPP, Radboud University Nijmegen, P.O. Box 9010, 6500 GL Nijmegen, The Netherlands*

²*Centre for Astrophysics Research, University of Hertfordshire, College Lane, Hatfield AL10 9AB*

³*Isaac Newton Group of Telescopes, Apartado de correos 321, E38700 Santa Cruz de La Palma, Tenerife, Spain*

⁴*Institut für Physik, Karl-Franzen Universität Graz, Universitätsplatz 5, 8010 Graz, Austria*

⁵*SUPA†, Institute for Astronomy, School of Physics, University of Edinburgh, Royal Observatory Edinburgh, Blackford Hill, Edinburgh, EH9 3HJ*

⁶*Institute of Astronomy, Madingley Road, Cambridge CB3 0HA*

⁷*Department of Physics, Faculty of Science, Naresuan University, Phitsanulok, 65000, Thailand*

⁸*Department of Physics, University of Warwick, Coventry, CV4 7AL, UK*

⁹*Harvard-Smithsonian Center for Astrophysics, Cambridge, MA 02138, USA*

ABSTRACT

We present a proper motion survey of the Galactic plane, using IPHAS data and POSS-I Schmidt plate data as a first epoch, that probes down to proper motions below 50 milliarcseconds per year. The IPHAS survey covers the northern plane ($|b| < 5^\circ$) with CCD photometry in the r , i and $H\alpha$ passbands. We examine roughly 1400 sq. deg. of the IPHAS survey area and draw up a catalogue containing 103058 objects with significant proper motions below 150 milliarcseconds per year in the magnitude range $13.5 < r' < 19$. Our survey sample contains large samples of white dwarfs and subdwarfs which can be identified using a reduced proper motion diagram. We also found several objects with IPHAS colours suggesting $H\alpha$ emission and significant proper motions. One is the known cataclysmic variable GD552; two are known DB white dwarfs and five others are found to be non-DA (DB and DC) white dwarfs, which were included in the $H\alpha$ emission line catalogue due to their lack of absorption in the $H\alpha$ narrow-band.

Key words: Astronomical data bases: Surveys – optical: stars – Astrometry and celestial mechanics: Astrometry – Stars

1 INTRODUCTION

The INT Photometric H α Survey (IPHAS, Drew et al., 2005) is a deep ($r < 21$), CCD based survey in three filters (r, i, H_{α}) covering 1800 sq. deg. of the northern Galactic Plane ($|b| < 5^{\circ}$). IPHAS forms part of the European Galactic Plane Surveys (EGAPS), which also includes the UKIRT Infrared Deep Sky Survey (UKIDSS) Galactic Plane Survey (Lawrence et al., 2007, Lucas et al. 2008) covering 1800 sq. deg. of the plane in J, H, K to a depth of $K=19$ and the UV EXcess survey (UVEX, Groot et al. in prep.). UVEX is planned to complement IPHAS by covering the same area but in u, g and HeI 5875Å with an additional r band epoch. These surveys also have upcoming southern counterparts. With the number density of stars highly concentrated on the Plane, IPHAS and EGAPS provide ideal tools to study a whole range of stellar and Galactic research topics. They have already yielded significant discoveries in fields such as cataclysmic variables (Witham et al., 2007), planetary nebulae (Mampaso et al., 2006, Wesson et al., 2008), young low mass objects (Valdivielso et al., 2009), star forming regions (Vink et al., 2008) and extinction in the Galactic plane (Sale et al., 2009). Large scale CCD-based astronomical surveys such as IPHAS provide accurate photometric and astrometric data on large numbers of astronomical objects. In addition to their main science goals, surveys such as EGAPS make their data public (see Gonzalez-Solares et al., 2008 for details on public IPHAS data) and they can be used by anyone in the astronomical community to pursue their own research aims. Combining IPHAS data with those from other surveys with different wavebands or epochs can lead to discoveries of variable objects and can also allow the parameter space of each object to be expanded to include not only magnitudes and positions but proper motions as well. Here we undertake the first comprehensive, optical, wide field survey to identify proper motions below 0.1 arcseconds per year in the Galactic Plane by cross-referencing the IPHAS database with SuperCOSMOS (Hambly et al., 2001) scans of the POSS-I plates taken in the 1950s. This gives us a proper motion baseline of approximately fifty years.

Early proper motion surveys utilised blink comparators and exceptional patience to in-

* E-mail: ndeacon@astro.ru.nl

† Scottish Universities' Physics Alliance

identify moving stars manually. The early manual work of Luyten is brought together in two samples, the Luyten Half-Arcsecond Survey (LHS, Luyten, 1979a) which catalogued 3561 objects with proper motions greater than half an arcsecond per year and the New Luyten Two Tenths Catalogue (NLTT, Luyten, 1979b) which contained 58845 objects with $\mu > 0.2$ arcseconds per year ($''/\text{yr}$). Both these surveys ran into difficulties in the Galactic Plane with the NLTT survey less than 50% complete for $|b| < 15^\circ$ at magnitudes fainter than $V=16$ (Lepine & Shara, 2005). The main modern computational study is that of Lepine (2008). They used a sophisticated algorithm to degrade POSS-II images to the same quality as the older POSS-I images. The two could then be subtracted and high proper motion stars identified. This survey is complete to $V=20$ and $\mu=0.15''/\text{yr}$. However the survey suffers from crowding in the Galactic Plane leading to a reduction in completeness. Lepine & Shara estimate they are only 80-90% complete down to $V=19$ within 15 degrees of the Galactic Plane. Fedorov et al. (2009) predict their upcoming catalogue will cover low proper motions in the Galactic Plane but will not provide a consistent proper motion range due to a varying maximum proper motion. Gould & Kollmeier (2004) used data from the Sloan Digital Sky Survey photographic plate data to produce a proper motion survey below 100 milliarcseconds per year. However this avoided the Galactic plane. The study of Folkes et al. (2007) attempts to fill in the Galactic Plane gap left by southern surveys such as Deacon & Hambly (2007), Pokorny et al. (2004) and Finch et al. (2007) (all of which avoid the Plane) by combining UKST and 2MASS data in a similar manner to Deacon & Hambly (2007) to identify candidate low mass stars and brown dwarfs from their proper motion.

2 METHOD

In order to plan our proper motion survey we had to first consider the datasets available. Two datasets are available for use as a first epoch, both having been scanned using the SuperCOSMOS plate scanning machine (Hambly et al. 2001). As well as the POSS-I plates, the newer, higher quality POSS-II plates with better emulsion sensitivity and improved resolution are also available. These provide better astrometric accuracy but a much shorter time baseline with respect to IPHAS (10-15 years compared to the IPHAS data versus the roughly 50 year epoch difference between IPHAS and POSS-I). However a shorter baseline means less contamination due to spurious pairings; $n_{\text{spurious}} \propto (\mu_{\text{max}} \Delta t)^2$, where n_{spurious} is the number of spurious pairings, μ_{max} is the maximum proper motion and Δt is the epoch

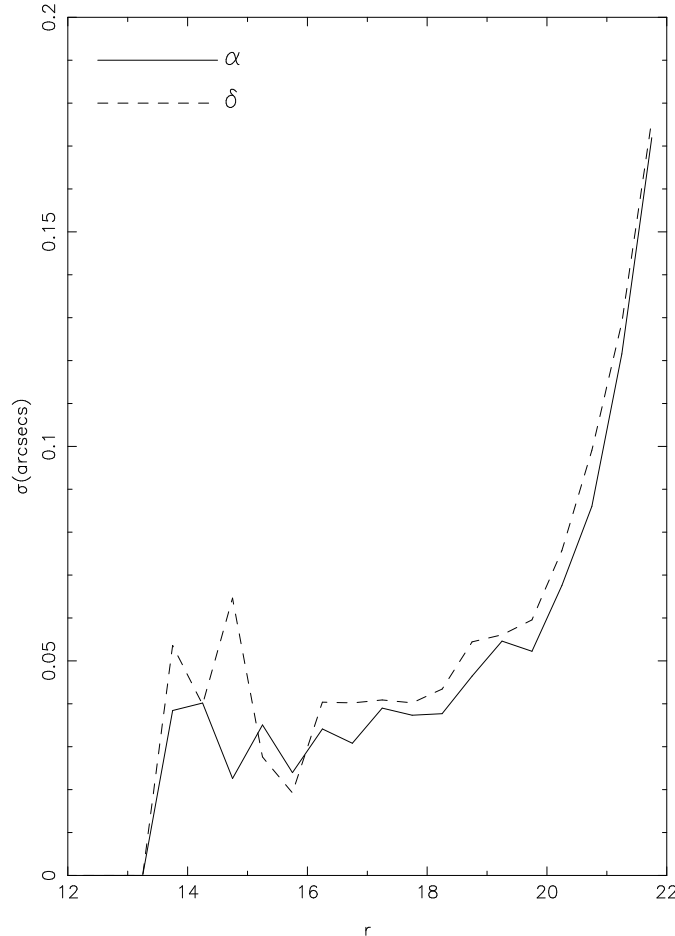


Figure 1. The astrometric errors (in arcseconds) between the IPHAS and UVEX surveys.

difference. n_{spurious} is also proportional to the density of objects around the target. This is one of the reasons most proper motion surveys have avoided higher density areas of the sky such as the Galactic Plane. Along with these data we also have the upcoming UV EXcess (UVEX) survey (Groot et al., in prep.) which will be a blue companion to IPHAS and a second r epoch. This will provide us with CCD quality second epoch astrometry, observed by the same telescope and camera, reduced by the same pipeline but with only a 3-5 year baseline. Examining the positional errors between IPHAS and UVEX we found that they were typically 40 milliarcseconds (see Figure 1), rising to 50 mas at $r=19$ (where POSS-I plate astrometry becomes difficult, see Figure 2) and to roughly 100 mas, as the survey limit ($r \sim 21$) is approached. Hence we can assume that with a three year baseline, the minimum 5σ proper motion detectable between IPHAS and UVEX at the survey limit ($r \sim 21$) is roughly 166 mas/yr. At the limit at which astrometry on the POSS-I plates becomes difficult ($R_F=19$) the minimum proper motion becomes 100 mas/yr. Hence below this latter limit (also below the $\mu=0.15''/\text{yr}$ lower proper motion limit of Lepine & Shara, 2008) there is

the potential for a lower proper motion survey to probe to previously unexplored proper motions in the Galactic Plane. To coincide with the lower limit of a potential IPHAS-UVEX proper motion survey (less than 100 mas/yr for objects brighter than $r=19$) and leaving some overlap we decided on a maximum proper motion of $0.15''/\text{yr}$. This means that even with the exceptionally long baseline between IPHAS and the POSS-I plates the maximum pairing radius is only $\sim 10''$, making spurious pairings unlikely. This is due not only to the low chance probability of another object lying in this region near to the target but also because many chance objects which lie so close to the target may also be deblended by the SuperCOSMOS software Hambly et al. (2001). For reasons of poor astrometry, we have excluded all deblended objects. The advantage of the POSS-II plates over the POSS-I plates is their better astrometry and photometry. However with the long IPHAS-POSS-I time baseline, even this better quality POSS-II astrometry cannot produce a lower minimum proper motion than using POSS-I plates and we have CCD quality photometry available from the IPHAS survey. The SuperCOSMOS scans of POSS-I plates only extend to $\delta \sim 2.5^\circ$, south of this we use SuperCOSMOS UK Schmidt Telescope R plates.

Before beginning the proper motion survey it is important to have both surveys on the same astrometric framework as our initial calculations will be based on the global astrometric frameworks of both surveys. IPHAS is tied to the 2MASS astrometric framework so we converted the POSS-I astrometry to the 2MASS astrometric reference frame. This was done in an identical way to the transformation of UKST I plates to the 2MASS system described in Section 2.1 of Deacon & Hambly (2007).

In order to estimate the minimum significant positional shift that can be detected we robustly calculated the positional errors between the POSS-I plates and the IPHAS survey (the error estimates calculated between the IPHAS and UVEX surveys found in Figure 1 were calculated in the same way). This was done by identifying the same objects in each epoch and calculating the positional differences. These were then binned by magnitude and the error calculated (Figure 2). After examining this plot, we determined the 5σ positional shift to be at one arcsecond, this was then used as our minimum positional shift. This means our minimum proper motion will be roughly 20 mas/yr. As we will calculate relative astrometric solutions for each object in our final catalogue this number may vary slightly.

Our search methodology was as follows. Objects which were flagged as stellar sources or probable stellar sources (classification flags -1 and -2, Drew et al., 2005) in IPHAS were selected. This excludes saturated sources and hence introduces a bright limit to our survey

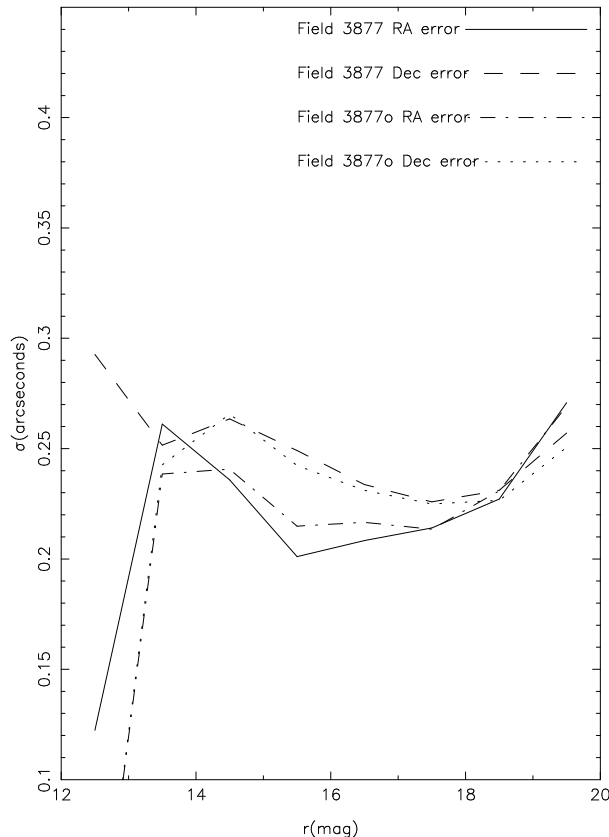


Figure 2. The astrometric errors (in arcseconds) between the IPHAS and POSS-I data.

at approximately $r=13.5$. One initial problem encountered was the difference in the sizes of the Point Spread Functions of the two surveys. Often two stars with a small separation which are resolved in IPHAS will be blended together on the lower resolution POSS plates leading to the erroneous conclusion that one or both of them have moved. To remove this potential source of contamination any IPHAS object of brightness $r = x$ (where x is in magnitudes) which had another IPHAS object brighter than $x - 2$ within 6 arcseconds was excluded. This magnitude difference was selected as typically objects which are two or more magnitudes fainter than an object will not significantly affect its astrometry. This pairing radius increased at brighter magnitudes, in line with the rough size of the POSS-I PSF (up to 20" for stars brighter than $r=9$).

Subsequently, IPHAS objects which were not affected by such crowding had their positions compared with the POSS-I data to see if they had a companion within an arcsecond. If they did they were judged not to have a significant proper motion and hence were excluded. Any potential POSS-I pair for these unpaired objects was then searched for. First

the region within $6''$ was searched and if no pair was found the region within $r_{max} = \mu_{max}\Delta t$ was searched. Any potential pair had to have a POSS-I R_F magnitude within 3σ (where σ is approximated from the values for measurement errors quoted in Hambly et al. 2001, roughly 0.2 magnitudes at best¹) of the IPHAS r magnitude and had to be stellar sources which had not been deblended and were not in close proximity to bright stars (note this 3σ cut could exclude high proper motion variables). To ensure that the paired POSS-I object does not have an IPHAS counterpart, the POSS-I positions were crosschecked with IPHAS positions and any object with an IPHAS pair within one arcsecond was excluded.

2.1 Calculation of astrometric solution

In order to gain an insight into the local astrometric accuracy of each proper motion measurement, a local relative astrometry mapping was carried out for each candidate. To do this all objects in the same IPHAS field as the target with brightnesses within one magnitude of the star in question were selected. These were then used to produce a 6 parameter plate-plate fit using *SlaLib* routines (Wallace, 1998) to determine the astrometric differences between the two reference frames and to estimate the random errors remaining once these differences have been corrected for. This fit was then applied and used to calculate a proper motion relative to this reference frame. This also yielded measures of the positional errors for each field. However in cases with few reference stars (i.e. <20) the error will be underestimated. To correct for this we carried out a series of simulations. Sets of reference stars on two different reference frames were created. These were given small random bulk offsets between the reference frames as well as individual random Gaussian errors. A fit between the reference frames was carried out and the calculated positional error compared to the individual positional errors used. It was found that for few reference stars the error was underestimated. We find that the correction factor is well fitted by the equation,

$$\frac{\sigma_{true}}{\sigma_{measured}} \approx 1 + \frac{19.8}{n_{ref}^{1.5}} \quad (1)$$

Where σ_{true} is the actual error, $\sigma_{measured}$ the measured error and n_{ref} the number of reference stars. We find this relation holds fairly well down to as few as six reference stars. This correction factor was used to ensure all our quoted errors are accurate. Where there were not enough reference stars for any fit an error calculated from the global positional error estimates shown in Figure 2 was used.

¹ Note as the IPHAS photometric errors are typically much smaller than POSS-I errors we ignore them in our error estimation.

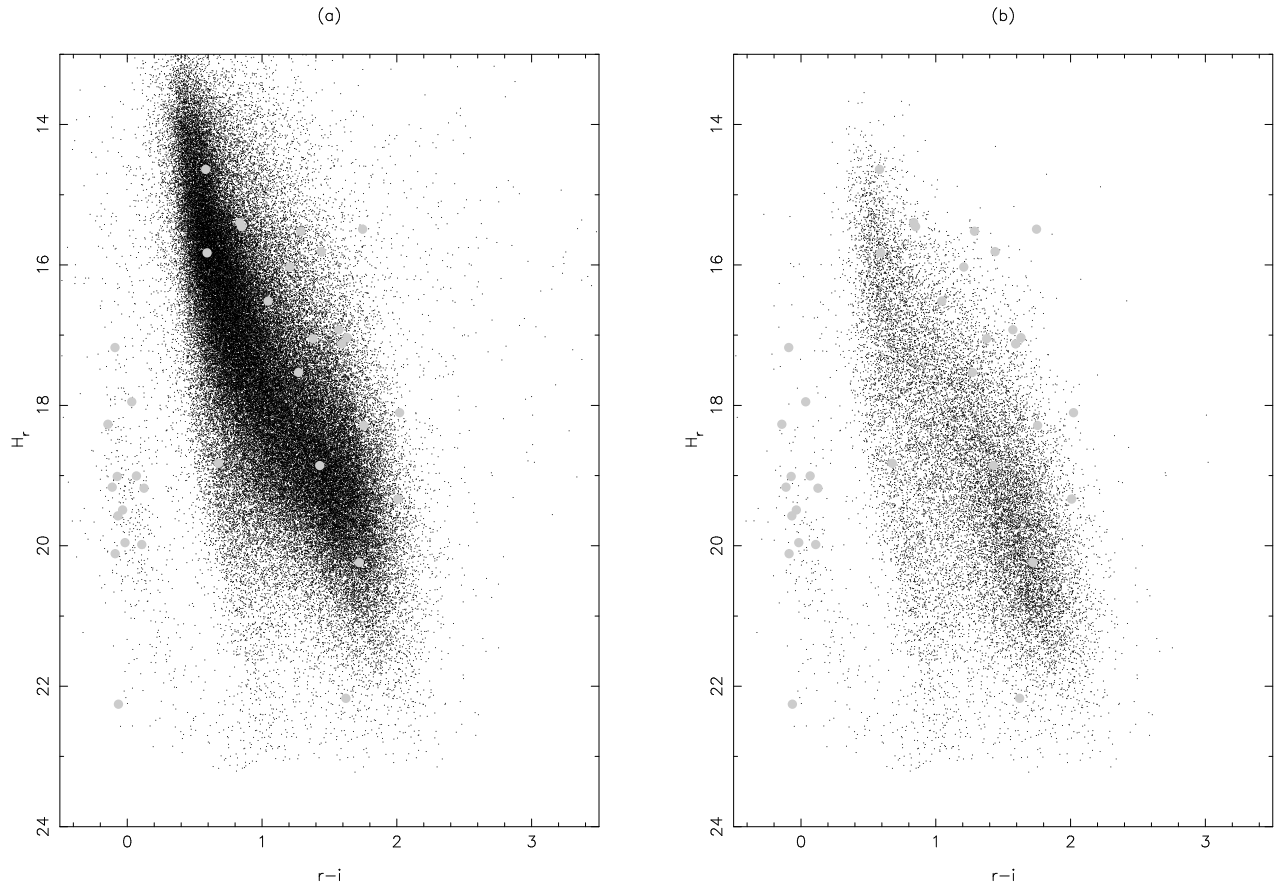


Figure 3. Two reduced proper motion diagrams for our dataset. (a) shows all objects in our sample, (b) shows only those with μ greater than 50mas/yr. The populations shown are as follows, the main locus is the main sequence, below and to the left are the higher velocity and bluer subdwarfs and to the left of them are the intrinsically fainter white dwarfs. The large grey dots represent the objects common between this catalogue and the catalogue of H_{α} emitters from Witham et al. (2008). These are all plotted on both panels, regardless of their proper motions.

3 RESULTS

The final catalogue consists of 103058 objects spread across 14126 IPHAS fields (including overlap fields) where the area of each field is roughly 0.3 sq.deg. These objects all have proper motions more significant than 5σ where the proper motion errors were typically below 10 milliarcseconds per year (i.e. $\mu_{min} < 40\text{mas}$). A full list of all these objects will be provided in the electronic edition. To check the sample a reduced proper motion diagram (Luyten, 1918, credited to Hertzsprung) was produced. Reduced proper motion takes observables (proper motion and apparent magnitude) and combines them in such a way that the result only depends on characteristics of the star (tangential velocity and absolute magnitude). The definition we use is given below.

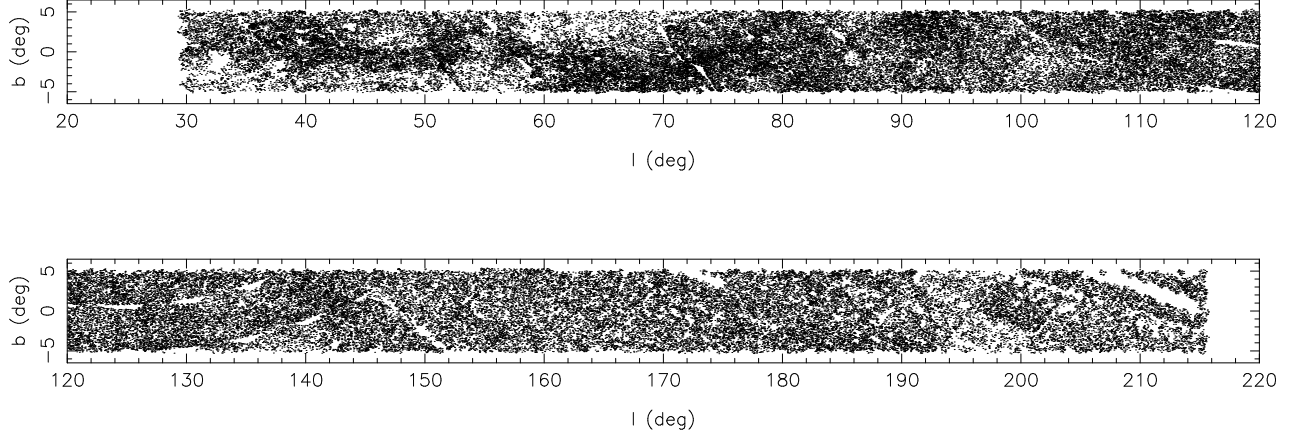


Figure 4. Distribution of objects in our sample across the Galactic plane. The coverage is in general good, however the coverage appears patchy in parts, particularly at low Galactic longitude ($l < 90$). Also note the areas with no coverage, these either lie outside the survey area (too far south) or have not yet been covered in the survey.

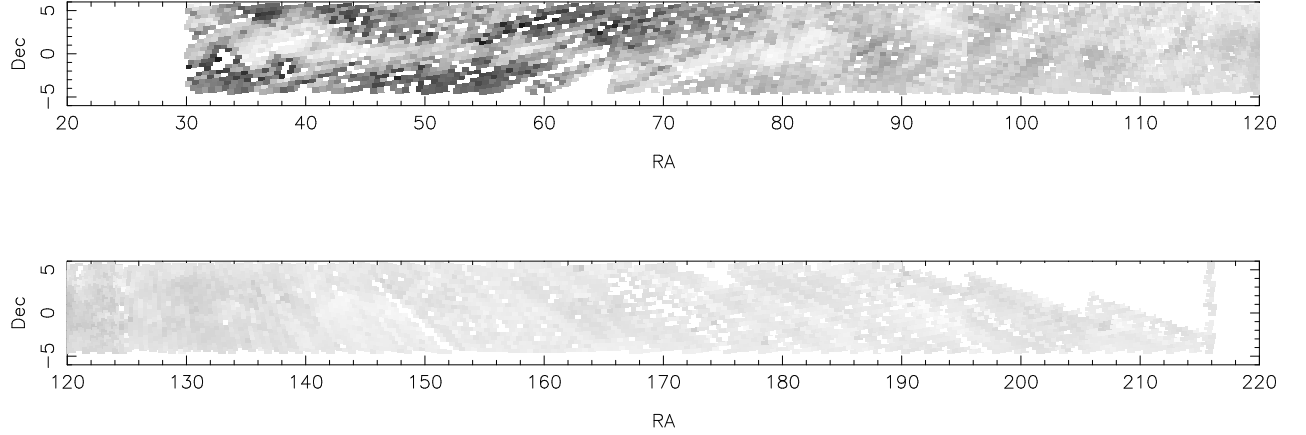


Figure 5. The density of stellar sources in the IPHAS survey with black being most dense and white being less dense. The larger stellar density closer to the Galactic centre along with the patches of extinction close to the plane in this region can be clearly seen.

$$\begin{aligned}
 H_r &= r + 5 \log_{10} \mu + 5 \log_{10}(47.4) \\
 H_r &= M_r + 5 \log_{10} d - 5 + 5 \log_{10} v_T - 5 \log_{10}(4.74) - 5 \log_{10} d + 8.379 \\
 H_r &= M_r + 5 \log_{10} v_T
 \end{aligned} \tag{2}$$

Where μ is the proper motion in arcseconds per year, d is the distance in parsecs and v_T is the tangential velocity in km/s. The above definition of reduced proper motion is not the most commonly used but is useful as it removes the constants needed to convert between units. Our reduced proper motion diagram is shown in Figure 3. The form is roughly what we would expect from a standard Galactic stellar population with clearly identifiable dwarf, subdwarf and white dwarf loci. However after we studied the spatial distribution of objects

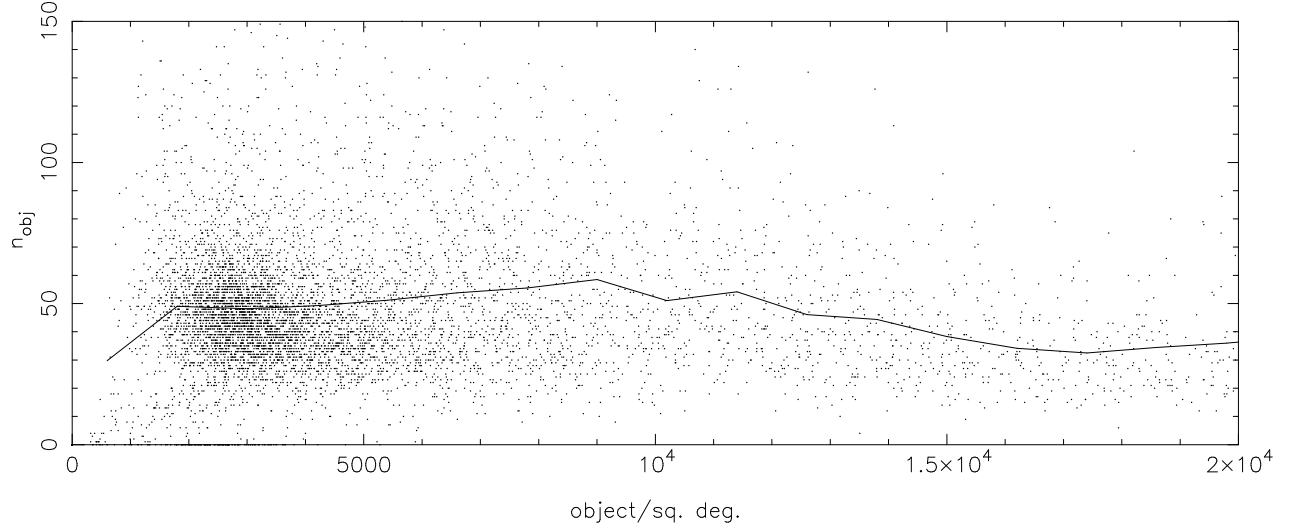


Figure 6. The density of stellar sources in the IPHAS survey for each field vs. the number of proper motion objects detected in each field. The solid line shows the mean number of objects for fields binned by stellar density. Note the general trend, dense fields have fewer detected objects. This is because the crowding confusion reduction algorithm removes more of the area of crowded fields.

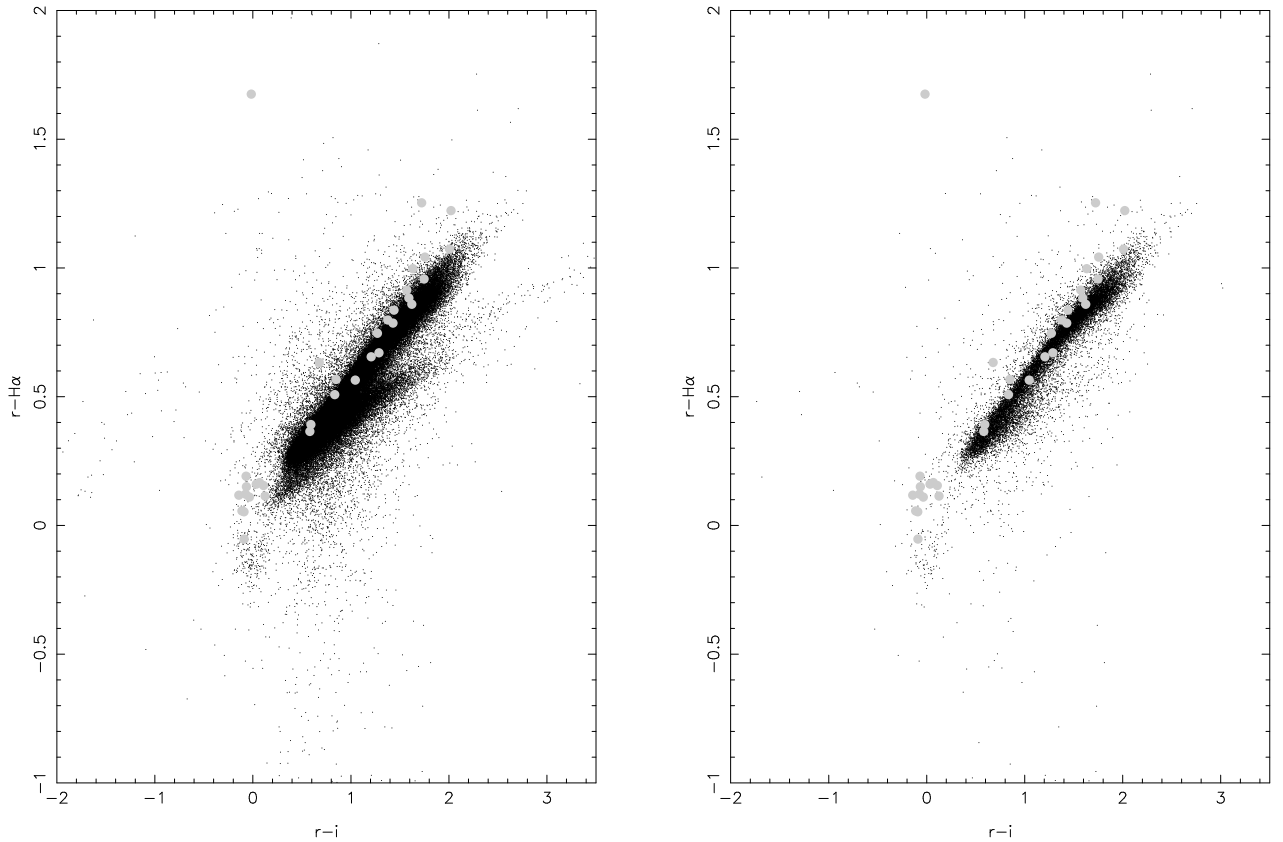


Figure 7. Colour-colour diagrams for the objects. The panel on the left (a) shows all the objects in our sample while the panel on the right (b) shows only those with proper motions greater than 50 mas/yr. The main stellar locus runs from (0.0, 0.1) to (2.0, 1.0), this is a near-perfect unreddened main sequence (see Drew et al., 2005). Below and to the left lie the bluer white dwarfs and above and to the left lie potential H α emitters. The large grey dots represent the objects common between this catalogue and the catalogue of H α emitters from Witham et al. (2008). These are all plotted on both panels, regardless of their proper motions.

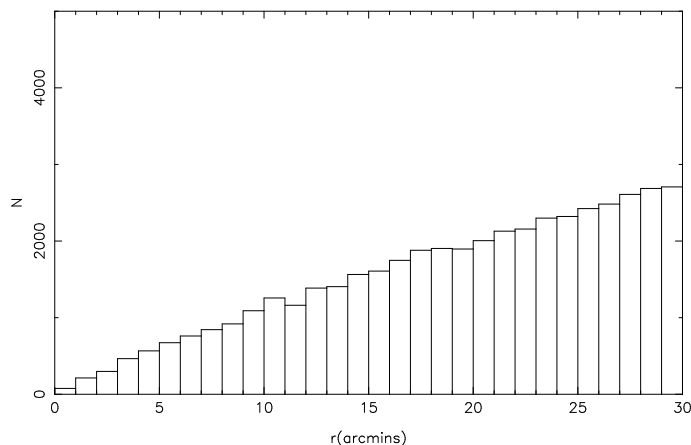


Figure 8. A histogram of the separations of common proper motion pairs in our sample. The trend for coincidence objects would be $N \propto r$. As we see no deviation from this trend at small separations, we conclude that there is no significant population of true common proper motion binaries in our sample.

it was found that there were several fields with many (more than 250) objects. After some investigation it became clear that these fields had poor astrometric solutions in the IPHAS data (mostly due to poor observing conditions). When we examined a histogram of number of detected objects per field it was found that these fields lay beyond the point where the main distribution had died away. Additionally when the reduced proper motion diagrams for objects in these fields was examined it was found that it did not contain the expected population distributions, indicating that the proper motion determinations were not correct. Hence any object lying in these fields was excluded from the final catalogue. A plot of the spatial distribution of the remaining objects can be found in Figure 4. It shows that for the majority of the northern plane, the coverage is good with a few patches of incompleteness. However moving along the plane towards the Galactic centre the number of objects drops off dramatically. This is due to our selection criteria excluding crowded regions as well as large numbers of objects in these regions being blended with other images (again a result of high stellar density). This can be seen in Figure 5 which shows the density of stellar sources in each IPHAS field: there are clearly fewer high proper motion objects detected in areas of higher stellar density ². This is also shown by the inverse correlation between the density of stellar sources in a field and the typical number of detected proper motion sources in that field (see Figure 6). Figure 7 shows an IPHAS colour-colour plot for our objects. The main locus is a clear, unreddened main sequence (see Drew et al., 2005), widened by the fact that

² The general trend towards more crowded fields towards the Galactic centre can be seen in Figure 3 of Gonzalez-Solares et al. 2008

the IPHAS photometry is not yet globally calibrated. Approximately 96% of objects in the catalogue lie on or close to this main sequence. There is also a white dwarf locus present lying below and to the left of the main sequence. Many objects lie above and to the left of the main sequence. While this may suggest $H\alpha$ emission, it may also be due to poor photometry in a particular field. Hence rather than select all these as potential $H\alpha$ emitters, in the next section we will use the study of Witham et al. (2008) to identify objects which appear to have significant $H\alpha$ emission relative to the main sequence on the particular field. Finally we checked our sample for common proper motion binaries. To investigate if we had a distinct population of common proper motion binaries, we plotted a histogram of the separations of all the objects with proper motions within 2σ of each other. The trend for coincidence objects should be $N \propto r$ and any excess above this at small separations would indicate a separate population of physically bound common proper motion objects. Figure 8 shows our histogram, clearly there is no distinct population of common proper motion binaries present.

3.1 Comparisons with other IPHAS studies

As stated earlier, the IPHAS survey is currently being exploited for many different scientific goals. One study utilising IPHAS photometry is that of Witham et al. (2008). Here IPHAS photometry is used to identify objects which lie significantly above the main stellar locus on a colour-colour diagram similar to Figure 7. As there will be offsets in the photometry from field to field, Witham et al. (2008) identifies potential $H\alpha$ emitters relative to the colour-colour diagram for the field the object lies in. Hence objects which appear to be $H\alpha$ emitters due to the poor photometry of an individual field are not included in Witham et al's sample. This allows us to treat this dataset as a clean sample of potential $H\alpha$ emitters. Cross-referencing this with our own proper motion sample will remove highly reddened (and distant) Be stars from the Witham sample and should leave only potential Cataclysmic Variables candidates, dMe stars and non-DA white dwarfs (ie. nearby stellar sources showing either $H\alpha$ emission or less than expected $H\alpha$ absorption). In this cross-referencing, we also included objects found in our study with proper motions between 0.2 and 0.15 arcseconds per year and objects with r magnitudes between 19 and 20. These were not included in the final catalogue as these objects were found to suffer from a high level of contamination.

The thirty six crossmatches are shown in Table 1. Note eight crossmatches were excluded from this list and from Figures 3 and 7 after inspection of the images by eye found that

Table 1. Objects common between our catalogue and the H α catalogue of Witham et al. (2008). IPHASJ225040+632838 is the known proper motion CV system GD 552 (Greenstein & Giclas 1978), IPHASJ043839+410931 is (GD 61 Giclas, Burham & Thomas, 1965), IPHASJ210951+425705 is EGGR 334 (Greenstein, 1974) and IPHASJ032825+580645 is the known high proper motion star LSPM J0328+5806 (Lepine & Shara, 2005). spectral type sources ¹ WHT spectroscopy, ² FAST spectroscopy, 3 Giclas, Burham & Thomas (1965), ⁴ Greenstein (1974), ⁵ Greenstein & Giclas 1978

Name	Position	μ_α "/yr	μ_δ "/yr	σ_{μ_α} "/yr	σ_{μ_δ} "/yr	r	i	H_α	SpT
IPHASJ000528+663951	00 05 28.05 +66 39 51.5	0.031	-0.051	0.009	0.009 ²	13.582	13.001	13.190	
IPHASJ002156+630635	00 21 56.62 +63 06 35.8	-0.044	-0.026	0.005	0.005 ²	17.105	17.183	16.993	
IPHASJ010749+582709	01 07 49.39 +58 27 09.3	0.022	-0.031	0.005	0.006 ²	14.171	13.279	13.657	
IPHASJ031119+600110	03 11 19.21 +60 01 10.8	0.044	-0.053	0.005	0.006 ¹	18.181	15.995	17.058	
IPHASJ032327+534705	03 23 27.39 +53 47 05.4	0.061	-0.054	0.005	0.005 ¹	16.734	16.980	16.576	
IPHASJ032825+580645	03 28 25.12 +58 06 45.8	0.144	-0.042	0.006	0.007 ²	17.684	17.917	17.550	
IPHASJ032905+563606	03 29 05.01 +56 36 06.8	-0.019	-0.034	0.006	0.007 ²	14.704	13.503	14.053	
IPHASJ033805+563518	03 38 05.68 +56 35 18.7	0.029	-0.038	0.006	0.006 ²	13.743	12.461	13.077	dMe ²
IPHASJ034042+573053	03 40 42.96 +57 30 53.7	0.069	-0.033	0.006	0.006 ²	13.724	12.685	13.164	dM ²
IPHASJ040147+540650	04 01 47.07 +54 06 50.8	0.044	-0.058	0.006	0.007 ²	16.122	14.727	15.361	
IPHASJ043839+410931	04 38 39.38 +41 09 31.9	-0.011	-0.110	0.005	0.006 ²	14.673	14.816	14.556	DB ³
IPHASJ045400+470031	04 54 00.68 +47 00 31.0	0.004	-0.023	0.006	0.003 ¹	17.723	17.691	17.563	
IPHASJ053015+251137	05 30 15.51 +25 11 37.3	0.031	0.044	0.005	0.005 ²	13.429	12.580	12.862	dM ²
IPHASJ055551+324150	05 55 51.14 +32 41 50.3	-0.037	-0.001	0.006	0.006 ²	17.829	17.707	17.599	DC ²
IPHASJ055752+274641	05 57 52.90 +27 46 41.8	0.025	-0.044	0.005	0.006 ¹	17.264	17.415	17.189	DC ²
IPHASJ061409+171136	06 14 09.36 +17 11 36.0	0.003	-0.044	0.006	0.006 ²	16.670	14.917	15.628	
IPHASJ062809+163158	06 28 09.40 +16 31 58.7	-0.046	-0.012	0.006	0.006 ²	17.833	17.909	17.642	DB ¹
IPHASJ183523+014245	18 35 23.26 +01 42 45.4	0.154	0.015	0.006	0.006 ²	17.700	16.172	16.921	
IPHASJ184306+004111	18 43 06.88 +00 41 11.3	-0.031	-0.048	0.005	0.005 ²	18.020	18.071	17.930	
IPHASJ185929-040304	18 59 29.38 -04 03 04.3	0.051	-0.027	0.005	0.005 ²	13.335	11.604	12.384	
IPHASJ190132+145807	19 01 32.77 +14 58 07.6	0.082	0.076	0.006	0.007 ¹	15.905	15.870	15.823	DC ²
IPHASJ190142-043621	19 01 42.09 -04 36 21.1	0.001	-0.034	0.007	0.006 ¹	15.999	14.622	15.201	
IPHASJ190338-025232	19 03 38.54 -02 52 32.4	0.032	-0.010	0.005	0.005 ¹	16.514	15.243	15.768	
IPHASJ191733+031937	19 17 33.35 +03 19 37.9	0.138	-0.032	0.005	0.006 ²	15.406	14.984	14.830	
IPHASJ192206+053238	19 22 06.11 +05 32 38.5	0.031	0.000	0.005	0.005 ²	16.254	14.723	15.450	
IPHASJ201409+265254	20 14 09.92 +26 52 54.1	0.035	0.038	0.005	0.006 ¹	15.113	13.408	14.187	
IPHASJ210541+534334	21 05 41.78 +53 43 34.5	0.025	-0.020	0.005	0.005 ²	14.891	13.451	14.055	
IPHASJ210923+515607	21 09 23.85 +51 56 07.8	0.027	0.038	0.006	0.006 ²	17.632	15.631	16.531	
IPHASJ210951+425705	21 09 51.24 +42 57 05.1	0.192	-0.018	0.010	0.005 ¹	15.552	15.559	15.340	DB ⁴
IPHASJ215029+554250	21 50 29.23 +55 42 50.6	0.027	0.006	0.005	0.005 ¹	17.477	15.492	16.283	
IPHASJ223541+590745	22 35 41.31 +59 07 45.7	0.026	-0.005	0.004	0.005 ¹	16.644	16.729	16.547	
IPHASJ224918+614903	22 49 18.57 +61 49 03.9	-0.039	-0.023	0.004	0.005 ²	17.508	17.475	17.436	DA ¹
IPHASJ225040+632838	22 50 40.03 +63 28 38.2	0.102	-0.037	0.005	0.006 ²	16.389	16.406	14.714	CV ⁵
IPHASJ232003+571736	23 20 03.28 +57 17 36.6	-0.035	0.000	0.007	0.007 ²	13.537	12.965	13.170	
IPHASJ232158+581034	23 21 58.03 +58 10 34.6	0.030	-0.011	0.006	0.005 ¹	16.037	14.454	15.129	
IPHASJ232908+615911	23 29 08.78 +61 59 11.0	-0.183	-0.067	0.007	0.004 ²	17.626	17.304	17.330	DC ¹

they may be blended objects. Examining Figure 7 we can see that many of the grey dots (representing Witham et al.’s H α emitters with significant proper motions) fall along the main sequence. It is possible that these are true H α emitters and appear in this part of the diagram due to uncorrected field to field photometric offsets or some selection effect. Of these objects one (IPHASJ053015+251137) appears to share a common proper motion with the nearby (separation 42") star TYC 1852-777-1 (Hog et al., 1998). The two proper motions agree within one sigma implying these are a true bound pair or part of the same moving group. Three other objects redder than $r - i = 0.4$ have spectra from FAST follow-up observations of IPHAS sources. Of these one (IPHASJ033805+563518) was found to be an M dwarf with H α emission. The question remains as to why these objects appeared in

Witham et al.’s catalogue. Witham et al. fitted a curve to the unreddened main sequence in each field and identified emitters as objects which lay significantly above this curve. The two non-emitting M dwarfs lie in the brightest selection bin of Witham et al.’s selection process ($r < 16$). Here the number of objects defining the unreddened main sequence will be smallest. It could be that these are marginal selections where the unreddened main sequence is affected by poor statistics. It is also possible that these are objects with variable weak $H\alpha$ emission. One moderately red object (IPHASJ191733+031937) appears to lie on the subdwarf sequence.

Fifteen of the cross matches objects which appear to lie on the white dwarf sequence in the reduced proper motion diagram (Figure 3). Of these IPHASJ225040+632838 is the low state CV system GD 552 (Greenstein & Giclas 1978). Another two, IPHASJ043839+410931 (GD 61, Giclas, Burham & Thomas, 1965) and IPHASJ210951+425705 (EGGR 334, Greenstein, 1974) are known DB white dwarfs. Additionally three objects had spectra taken in the IPHAS spectroscopic follow-up programme with the FAST spectrograph on the 1.5m Tillinghast telescope on Mount Hopkins. Of the remaining nine objects, three had spectra taken using the ISIS spectrograph on the William Herschel Telescope (WHT) on La Palma. These spectra were used to provide rough spectral classifications which can be found in Table 1. Seven of the eight spectrally classified objects which lie bluewards of $r - i = 0.4$ in the colour-colour diagram (excluding the known CV GD 552) are non-DA white dwarfs. Hence we believe the remaining objects are good non-DA white dwarf candidates.

Valdivielso et al. (2008) have produced a sample of young, low mass objects using IPHAS data. Clearly identifying the proper motions of such objects could establish a connection with a known star forming association or moving group. Unfortunately none of these objects appear in our catalogue.

4 DISCUSSION

In order to provide a rough estimate of our completeness, we plotted a cumulative proper motion histogram. This is shown in Figure 9. Assuming uniform spatial and velocity distributions and a fully complete survey, the distribution should scale as $N \propto \mu^{-3}$. This is represented by the solid line in the plot. It is clear that we begin to become incomplete below 60 milliarcseconds per year. This is due to a combination of our limiting magnitude and some objects falling in fields with poor astrometry (hence having proper motions which are

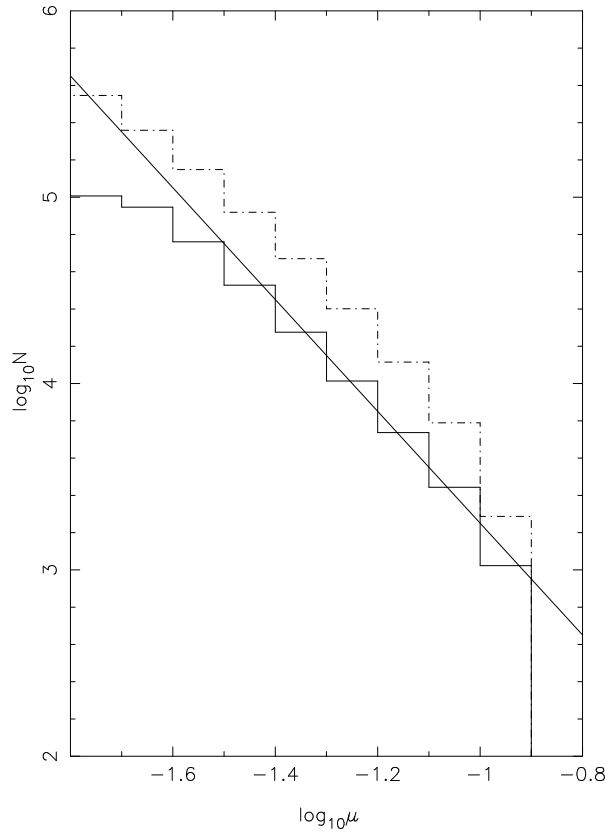


Figure 9. A cumulative proper motion histogram for our the objects in our catalogue. The solid line represents the $N \propto \mu^{-3}$ relation that would be expected with no incompleteness. It is clear that our survey begins to become incomplete below about 60 milliarcseconds per year and that below 20 milliarcseconds per year there are virtually no objects. The dotted line represents the study of Gould & Kollmeier (2004). Clearly their study is complete to lower proper motions than ours. In the region where our survey is most complete there is a factor of 2 difference between the numbers.

not significant enough). Below about 25 mas/yr it is clear the distribution flattens off and we can say we have no significant population below this mark. We have also compared our results with those in Gould & Kollmeier (2004). Figure 9 shows that in the proper motion range where both surveys have similar proper motion completeness, we have half the number of objects that Gould & Kollmeier have. This is despite the two surveys having similar areas (both around 1400 sq. deg.). However our survey covers a much more crowded area than theirs. Deacon, Hambly & Cooke (2005) calculated the area lost to bright and blended stars across the southern sky. Examining their Figure 10, it is clear that in the southern regions of the sky at similar Galactic latitude to ours, the completeness is often 50% or worse. Hence we believe this difference in numbers is due the more crowded nature of our survey area.

The IPHAS survey consists of 15270 pointings, which between them cover the 1800 square-degree survey area twice or more. Hence simply taking the size of the detector and multiplying it by the number of fields our survey covers (12362) will not yield an accurate estimate of our current survey area. A rough estimate can be provided by multiplying the fraction of the fields we cover (approximately 81%) by the total final survey area of 1800

sq. deg. This yields and approximate area for our proper motion survey of 1457 sq. deg. However as stated above, due to crowding we are only likely to identify proper motion objects in roughly half this total area. Once data from the few unobserved IPHAS fields have been released we will apply the same method to the remaining fields, completing our proper motion survey.

In calculating our astrometric solutions we use sets of reference stars. These may have small bulk motions. Additionally for the objects where we have too few reference stars the raw IPHAS positions are used. These are tied to the 2MASS (Skrutskie et al. 2006) system using reference stars. Hence we will measure proper motions relative to these reference stars rather than absolute proper motions. Lepine (2008) also encountered this problem. They concluded that the difference between absolute and relative proper motions was typically less than their measurement errors. As our measurement errors are similar to theirs (typically below their quoted global errors of 8mas/yr in each axis), we deduce that any offset between the relative and absolute proper motions of our sample will also be below our calculated errors.

5 CONCLUSIONS

We have completed the first comprehensive wide field proper motion survey of the northern Galactic plane ($|b| < 5^\circ$) covering proper motions between 150 and approximately 30 arcseconds per year. This sample covers a large section (1457 sq. deg.) of the northern plane and contains 57249 objects with significant proper motions. We also identify seventeen objects in common between our catalogue and the H α emission catalogue of Witham et al. (2008). These objects fell in to two distinct groups, a blue group dominated by non-DA white dwarfs and a red group dominated by marginally selected ordinary main sequence objects. This sample will clearly be useful in the study of populations such as white dwarfs and subdwarfs in the Galactic plane. We will seek to complete the catalogue for the full survey area and will use the upcoming UVEX data to extend it to higher proper motions above the current imposed limit of 0.15 arcseconds per year.

ACKNOWLEDGMENTS

This paper uses data from the SuperCOSMOS Sky Survey and from the INT Photometric H α Survey of the northern Galactic plane (IPHAS) carried out at the Isaac Newton Telescope

(INT). The INT is operated on the island of La Palma by the Isaac Newton Group in the Spanish Observatorio del Roque de los Muchachos of the Instituto de Astrofísica de Canarias. All IPHAS data are processed by the Cambridge Astronomical Survey Unit, at the Institute of Astronomy in Cambridge.. N.R.D. is funded by NOVA and by NWO-VIDI grant 639.041.405 to Paul Groot. DS acknowledges a STFC Advanced Fellowship. This paper makes use of Slalib routines (see Wallace, 1998). This research has made use of the SIMBAD database, operated at CDS, Strasbourg, France. We thank the FAST observers for their assistance with obtaining the follow-up spectroscopy of IPHAS emitters. The 1.5m Tillinghast telescope is located near Mt.Hopkins in Arizona and operated on behalf of the Smithsonian Astrophysical Observatory. the authors would like to thank Boris Gaensicke, Christian Knigge, Quentin Parker and Stuart Sale for their helpful comments.

REFERENCES

- Deacon, N.R., Hambly, N.C., Cooke, J.A., 2005, *A&A*, 435, 363
- Deacon, N.R., Hambly, N.C., 2007, *A&A*, 468, 163
- Drew, J.E., Greimel, R., Irwin, M.J., et al., 2005, *MNRAS*, 362, 753
- Fedorov, P.N., Myznikov, A.A., Akhmetov, V.S., 2009, *MNRAS*, 393, 133
- Finch, C.T., Henry, T.J., Subasavage, J.P., et al., 2007, *AJ*, 133, 2898
- Folkes, S.L., Pinfield, D.J., Kendall, T.R., Jones, H.R.A., 2007, *MNRAS*, 378, 901
- Giclas, H.L., Burnham, R., Thomas, N.G., 1965, *LowOB*, 6, 155
- Gonzalez-Solares, E.A., Walton, N.A., Greimel, R., et al., 2008, 2008, *MNRAS*, 388, 89
- Gould, A., Kollmeier, J.A, 2004, *ApJS*, 152, 103
- Greenstein, J.L., Giclas, H., 1978, *PASP*, 90, 460
- Greenstein, J.L., 1974, *ApJ*, 189, 131
- Groot, P.J., et al., in prep.
- Hambly, N.C., MacGillivray, H.T., Read, M.A., Tritton, S.B., Thomson, E.B., Kelly, B.D., Morgan, D.H., Smith, R.E., Driver, S.P., Williamson, J., Parker, Q.A., Hawkins, M.R.S., Williams, P.M., Lawrence, A., *MNRAS*, 326, 4, 1279, 2001
- Hog, E., et al., 1998, *A&A*, 335, 65
- Lawrence, A., Warren, S.J., Almaini, O., et al., 2007, *MNRAS*.379, 1599
- Lepine, S., Shara, M.M., 2005, *AJ*, 129, 3, 1483
- Lepine, S., 2008, *AJ*, 135, 2177

[h]

Table A1. An example of the data tables available electronically for this paper.¹ indicates astrometric solutions calculated from reference stars, ² implies the astrometric errors are drawn from global error estimates. The Modified Julian date (MJD) and the position are both taken from the IPHAS observations.

Name	Position J2000	μ_α "/yr	μ_δ "/yr	σ_{μ_α} "/yr	σ_{μ_δ} "/yr	r	i	H α	MJD
IPHASJ000001+575210	00 00 01.48 +57 52 10.9	-0.009	-0.034	0.008	0.004 ²	15.278	14.700	14.956	53666
IPHASJ000001+652057	00 00 01.81 +65 20 57.0	0.002	-0.029	0.007	0.005 ²	14.995	14.214	14.627	53664
IPHASJ000005+644818	00 00 05.67 +64 48 18.2	-0.001	-0.044	0.006	0.005 ²	18.923	17.575	18.455	53664
IPHASJ000005+602518	00 00 05.81 +60 25 18.0	0.036	0.010	0.005	0.005 ¹	17.328	16.598	16.927	53665
IPHASJ000009+652017	00 00 09.09 +65 20 17.2	-0.078	0.008	0.007	0.006 ²	19.885	18.113	19.235	53664
IPHASJ000010+602519	00 00 10.07 +60 25 19.7	-0.059	-0.025	0.009	0.007 ²	13.659	12.837	13.184	53666
IPHASJ000013+582109	00 00 13.26 +58 21 09.5	-0.032	-0.029	0.007	0.004 ²	17.388	15.783	16.565	53665
IPHASJ000014+631007	00 00 14.91 +63 10 07.1	0.035	-0.004	0.006	0.006 ¹	16.513	15.365	15.879	53666
IPHASJ000017+664726	00 00 17.51 +66 47 26.4	-0.023	-0.05	0.006	0.006 ²	12.748	12.328	12.519	54009
IPHASJ000017+620139	00 00 17.51 +62 01 39.0	0.037	-0.001	0.007	0.008 ¹	17.660	15.958	16.761	53244
IPHASJ000018+592623	00 00 18.76 +59 26 23.4	0.072	-0.027	0.004	0.007 ¹	16.140	14.542	15.308	53666
IPHASJ000023+661414	00 00 23.88 +66 14 14.3	0.038	0.005	0.005	0.007 ¹	17.770	16.107	16.977	53666

Lucas, P.W., Hoare, M.G., Longmore, A., et al., 2008, MNRAS, 391, 136

Luyten, W.J., 1918, Lick Observatory Bulletin, vol. 10, pp.135-140

Luyten Half Arcsecond Catalogue, Luyten, W.J., University of Minnesota, Minneapolis, 1979

New Luyten Two Tenths Catalogue, Luyten, W.J., University of Minnesota, Minneapolis, 1979

Mampaso, A., Corradi, R.L.M., Viironen, K., et al., 2006, A&A, 458, 203

Pokorny, R.S., Jones, H.R.A., Hambly, N.C., 2003, A&A, 397, 575

Sale, S.E., Drew, J.E., Unruh, Y.C., 2009, MNRAS, 392, 497

Skrutskie, M.F., Cutri, R.M., Stiening, R., et al., 2006, AJ, 131, 1163

Valdivielso, L., Martin, E.L., Bouy, H., et al., 2009, A&A, 497, 973

Vink, J.S., Drew, J.E., Steeghs, D., et al., 2008, MNRAS, 387, 308

Wallace, P.T., Starlink User Note No. 67.42: SLALIB: Positional Astronomy Library, CCLRC/Rutherford Appleton Laboratory, PPARC, 1998

Wesson, R., Barlow, M.J., Corradi, R.L.M., 2008 ApJ, 688, 21

Witham, A.R., Knigge, C., Drew, J.E., et al., 2008, MNRAS, 384, 1277

APPENDIX A: EXAMPLE DATA TABLE

The data tables for this paper will be available electronically. Here we give an example of one of the data tables.